Rapid Turnover of T Lymphocytes in SIV-Infected Rhesus Macaques

Hiroshi Mohri, Sebastian Bonhoeffer, Simon Monard, Alan S. Perelson, David D. Ho*

Studies of lymphocyte turnover in animal models have implications for understanding the mechanism of cell killing and the extent of lymphocyte regeneration in human immunodeficiency virus infection. Quantitative analyses of the sequential changes in bromodeoxyuridine labeling of CD4 and CD8 T lymphocytes not only revealed the normal proliferation and death rates of these cell populations in uninfected macaques, but also showed a substantial increase in these rates associated with simian immunodeficiency virus (SIV) infection. Faster labeling and delabeling in memory and naïve T lymphocyte subpopulations as well as in NK (natural killer) and B cells were also observed in infected macaques, suggesting a state of generalized activation induced by SIV.

Human immunodeficiency virus–1 (HIV-1) replication in infected persons is continuous, with a rapid turnover of virions and productively infected CD4 lymphocytes (*1*). A recent study has shown similar viral kinetics in rhesus macaques infected by SIV (*2*). To maintain a dynamic equilibrium, the loss of infected cells must be continuously replaced by de novo infection of susceptible CD4 lymphocytes (*1*, *3*). By quantifying the rebound in CD4 T cell counts during potent antiretroviral therapy in patients, a turnover rate of 1×10^9 to 2×10^9 cells/day was determined (*1*), although a normal rate was not available for comparison. However, this estimate of lymphocyte turnover would be too high if the CD4 cell rebound was largely due to lymphocyte redistribution rather than production (*4*). But recent studies have found CD4 lymphocyte expansion in both blood and lymphoid tissues in patients started on effective antiretroviral therapy (*5*), suggesting that cellular redistribution is only part of the explanation for the lymphocyte rise during treatment. Nevertheless, some have argued strongly against a rapid turnover of CD4 lymphocytes during HIV-1 infection, based on the stability of telomere length in CD4 T cells of infected persons (*6*). To better quantify lymphocyte dynamics in vivo, we conducted a study in normal and SIV-infected rhesus macaques, using the incorporation of the nucleoside analog bromodeoxyuridine (BrdU) to mark proliferating lymphocytes as well as to track their subsequent fate.

Sixteen adult rhesus macaques (age range of 8.0 to 18.5 years, mean of 14.0 years; weight range of 5.6 to 10.4 kg, mean of 7.7 kg), including four uninfected and 12 infected with SIVmac251, were used for this study (Table 1). Five infected monkeys had relatively low plasma viral load (≤20,000 RNA copies per milliliter), whereas seven had high levels (≥140,000 RNA copies per milliliter). For the first 3 weeks of the experiment, BrdU (Sigma) was placed in the drinking water (0.5 mg/ml), and its intake was carefully recorded for each animal. During this labeling phase, BrdU was incorporated into the DNA of proliferating cells. No toxicity was observed clinically or by routine laboratory testing. Blood samples were taken at weeks 0, 1, 2, and 3; lymph node biopsies and bone marrow aspirations were also performed on each macaque at week 3. Thereafter, all monkeys were placed back on normal drinking water, and during this delabeling phase of the experiment, blood samples were collected at weeks 4, 5, 6, 7, and 10.

Mononuclear cells from blood were isolated by Ficoll-Hypaque centrifugation for analysis. Cell-surface staining was first performed with monoclonal antibodies specific for CD3, CD4, CD45RA, CD20, and CD16 (*7*), followed by staining with a monoclonal antibody to BrdU conjugated to fluorescein isothiocyanate (FITC; Becton Dickinson) (*8*) before flow cytometric analysis.

That the rapidly growing myeloid cells from the bone marrow were on average 87% BrdU-positive (BrdU+) suggests adequate signal uptake into proliferating cells in each macaque. BrdU incorporation was also observed in T lymphocytes in blood and lymph node, albeit at a lower percentage. Labeled cells were readily quantified into blood $CD3^+CD4^+$ and $CD3^+CD4^-$ lymphocytes, with either the "naïve" ($CD45RA^+$) or "memory" ($CD45RA^-$) phenotype. At the end of the labeling period, the fraction of blood $CD3^+CD4^+$ and $CD3^+CD4^-$ lymphocytes that were BrdU+ was quite similar to that found in the corresponding cell populations in the lymph node (*9*), suggesting that the kinetics of cell labeling in blood is similar to that in lymphoid tissues. Thus, all sequential studies were performed only on blood samples.

In each macaque, the percentage of BrdU+ cells among $CD3^+CD4^+$ and $CD3^+CD4^-$ lymphocytes increased during the labeling period and declined thereafter. The rise and fall of BrdU positivity in both cell populations were most dramatic for the infected monkeys with high viral load, intermediate for the infected monkeys with low viral load, and lowest for the normal monkeys (Fig. 1A). In general, this pattern was representative of results obtained from the three different groups of experimental animals. Qualitatively, it is intuitive that a high labeling rate followed by rapid decay rate suggests faster turnover of the cell population. For the past two decades, results of BrdU labeling and decay experiments have been analyzed by comparing the slope of the rise in labeled cells as well as the slope of the loss of such cells (*10*). However, the values of these slopes do not directly reflect a particular biologic property of the cell population under study; instead, they represent a composite property of the population's proliferation rate and death rate. To obtain more explicit information, we developed a mathematical model that could yield estimates of proliferation and death rates.

The number of cells in the $CD4^+$ and $CD4^-$ T cell subpopulations can change by cell proliferation, cell death, and input of cells from a source (Fig. 2). The source represents replenishment of T cells by the thymus, extrathymic sites, or a subpopulation of peripheral T cells that can be recruited into active division (*11*). We assume that each cell population is at steady state before BrdU labeling and that labeling is not toxic. We further assume that once BrdU is introduced, the progenies of all dividing cells are labeled (*12*). After BrdU is introduced, we propose that the number of unlabeled cells, U, and labeled cells, L, changes as follows

$$dU/dt = s_U - pU - dU \quad (1a)$$

$$dL/dt = s_L + 2pU + pL - dL \quad (1b)$$

where p and d are the proliferation and death rates per cell, respectively, s_U and s_L are the rates of entry of unlabeled and labeled cells into the subpopulation from the source, and the factor of 2 in Eq. 1b reflects the assumption that, on division, an unlabeled cell gives rise to two labeled progenies. After time T, the end of BrdU administration at week 3, we assume the progenies

H. Mohri, S. Bonhoeffer, S. Monard, D. D. Ho, Aaron Diamond AIDS Research Center, The Rockefeller University, 455 First Avenue, New York, NY 10016, USA.
A. S. Perelson, Theoretical Division, Los Alamos National Laboratory, Los Alamos, NM 87545, USA.

*To whom correspondence should be addressed. E-mail: dho@adarc.org

Table 1. Baseline characteristics of uninfected and SIV-infected rhesus macaques, and a summary of the proliferation and death rates of their T lymphocytes. Proliferation and death rates were estimated using nonlinear least-squares regression. The subroutine DNLS1 from the Common Los Alamos Software Library, which is based on the Levenberg-Marquardt algorithm, was used to minimize the sum of the squared differences between the theoretical and measured values for each data point. Lower and upper 68% confidence bounds were calculated by a bootstrap method (*29*) and are shown in parentheses. Some estimates of p are listed as zero. This only implies that the rounded estimate is <0.001. Because we only labeled with BrdU for 3 weeks, our method cannot detect cells that divide very infrequently. Furthermore, the theoretical model as described by Eq. 3 is based on the assumption that labeling of dividing cells is 100% effective. If this is not the case, then the estimate of p will underestimate the true proliferation rate. ND, not done.

Macaques	Baseline values		BrdU intake (mg/kg/day)	Proliferation rate, p (day^{-1})	
	Plasma Virions* (10^3 per ml)	CD4 cells (per μl)		$CD3^+CD4^+$	$CD3^+CD4^-$
Uninfected					
Rh 1372	ND	1562	41	0.003 (0.002–0.003)	0.001 (0.000–0.002)
Rh 1426	ND	1801	43	0.000 (0.000–0.014)	0.000 (0.000–0.012)
Rh 1466	ND	1017	60	0.000 (0.000–0.013)	0.000 (0.000–0.009)
Rh 1458	ND	848	63	0.001 (0.000–0.011)	0.003 (0.002–0.003)
Mean ± SE		1307	52	0.001 ± 0.0006	0.001 ± 0.0006
Weighted mean‡ ± SE				0.003 ± 0.0005	0.002 ± 0.0090
Infected (low)					
Rh 1394	<10	1180	39	0.022 (0.006–0.038)	0.004 (0.000–0.020)
Rh 1294	<10	906	37	0.001 (0.000–0.023)	0.000 (0.000–0.017)
Rh 1380	<10	900	33	0.009 (0.000–0.021)	0.000 (0.000–0.013)
Rh 1436	<10	404	60	0.000 (0.000–0.020)	0.000 (0.000–0.011)
Rh 1324	20	953	40	0.013 (0.007–0.019)	0.017 (0.004–0.026)
Mean ± SE		869	42	0.009 ± 0.0042	0.004 ± 0.0032
Weighted mean ± SE				0.011 ± 0.0057	0.003 ± 0.0051
Infected (high)					
Rh 1314	140	295	31	0.000 (0.000–0.053)	0.001 (0.000–0.042)
Rh 1316	450	568	58	0.025 (0.015–0.038)	0.015 (0.007–0.025)
Rh 1292	530	690	35	0.038 (0.031–0.061)	0.068 (0.047–0.098)
Rh 1442	1200	668	54	0.000 (0.000–0.021)	0.000 (0.000–0.017)
Rh 1284	1500	366	59	0.000 (0.000–0.018)	0.000 (0.000–0.019)
Rh 1296	1900	296	42	0.107 (0.064–0.728)	0.040 (0.023–0.063)
Rh 1348	2200	391	65	0.050 (0.020–0.089)	0.038 (0.023–0.051)
Mean ± SE	1131	468	49	0.031 ± 0.0147†	0.023 ± 0.0099†
Weighted mean ± SE				0.010 ± 0.0104	0.015 ± 0.0090

of labeled cells remain labeled because BrdU+ chromosomes segregate independently into daughter cells (*13*). Thus, after BrdU administration is stopped

$$dU/dt = s'_U + pU - dU \quad (2a)$$

$$dL/dt = s'_L + pL - dL \quad (2b)$$

where s'_U and s'_L are the rates of entry of unlabeled and labeled cells into the subpopulation from the source during the delabeling phase. Solving Eqs. 1 and 2, we find that the fraction of labeled cells, f_L, is to a good approximation given by

$$f_L(t) = C\,(1 - e^{-(p+d)t}), \text{ if } t \le T$$

$$f_L(t) = C\,(1 - e^{-(p+d)T})e^{-(d-p)(t-T)}, \text{ if } t \ge T \quad (3)$$

where C is a constant (*14*).

By least-squares regression, the nonlinear Eq. 3 fitted the data for $CD3^+CD4^+$ and $CD3^+CD4^-$ lymphocytes, thereby yielding estimates of p and d for each cell population (Fig. 1A). Results for each macaque were analyzed in this fashion, and parameter estimates were obtained (Table 1). For the normal monkeys, the mean values of p (day^{-1}) were 0.001 ± 0.0006 and 0.001 ± 0.0006 for $CD3^+CD4^+$ and $CD3^+CD4^-$ populations, respectively; mean values of d (day^{-1}) were higher, 0.010 ± 0.0023 and 0.011 ± 0.0013, respectively. Compared to these values, estimates of p and d were several-fold higher for SIV-infected monkeys with low viral load; estimates were even higher for infected monkeys with high viral load. The estimates of p had broad 68% confidence intervals (see Table 1 legend), thus statistically significant differences were achieved only by comparing normal macaques with those with high viral load. By contrast, values of d had smaller 68% confidence intervals, and statistical significance was obtained when comparing normal animals to any infected group. Taken together, the results indicate that the turnover of $CD3^+CD4^+$ and $CD3^+CD4^-$ lymphocyte populations is substantially higher in SIV-infected macaques compared with normal animals.

Rates of BrdU labeling and delabeling were also determined in additional cell populations, including $CD3^+CD4^+$ and $CD3^+CD4^-$ T lymphocytes that were either $CD45RA^+$ (naïve) or $CD45RA^-$ (memory). $CD3^-CD8^+CD16^+$ (NK) and $CD3^-CD20^+$ (B lymphocytes) cells were examined as well. Results from three examples are shown in Fig. 1B. Findings in $CD3^+CD4^+$ and $CD3^+CD4^-$ populations were quite similar, and $CD45RA^-$ subpopulations were turning over faster than $CD45RA^+$ subpopulations. For each cell type shown in Fig. 1B, the labeling and delabeling rates were highest for infected macaques with high viral load and lowest for normal macaques. The mathematical model described above may not be appropriate to describe these populations, partly because of the interconversion of cells between $CD45RA^+$ and $CD45RA^-$ T lymphocytes (*15*) and the different population dynamics of B and NK cells. Therefore, only qualitative analyses were performed. The mean values of the downslopes of the regression lines during the delabeling phase (*16*) were determined for each group of experimental animals (Table 2). These numbers demonstrate that $CD45RA^-$ sub-

Table 1. (continued)

Macaques	Death rate, d (day^{-1})		Percent replacement (day^{-1})	
	$CD3^+CD4^+$	$CD3^+CD4^-$	$CD3^+CD4^+$	$CD3^+CD4^-$
Uninfected				
Rh 1372	0.005 (0.004–0.005)	0.007 (0.006–0.008)	0.2	0.6
Rh 1426	0.009 (0.009–0.021)	0.011 (0.010–0.023)	0.9	1.1
Rh 1466	0.016 (0.014–0.028)	0.012 (0.012–0.020)	1.6	1.2
Rh 1458	0.009 (0.008–0.018)	0.013 (0.012–0.014)	0.8	1.0
Mean ± SE	0.010 ± 0.0023	0.011 ± 0.0013	0.9 ± 0.3	1.0 ± 0.1
Weighted mean‡ ± SE	0.005 ± 0.0110	0.010 ± 0.0021		
Infected (low)				
Rh 1394	0.042 (0.028–0.059)	0.017 (0.012–0.033)	2.0	1.3
Rh 1294	0.011 (0.011–0.033)	0.012 (0.012–0.027)	1.0	1.2
Rh 1380	0.030 (0.024–0.042)	0.016 (0.015–0.029)	2.1	1.6
Rh 1436	0.044 (0.042–0.064)	0.026 (0.025–0.036)	4.4	2.6
Rh 1324	0.031 (0.026–0.037)	0.045 (0.036–0.055)	1.8	2.8
Mean ± SE	0.032 ± 0.0059†	0.023 ± 0.0058†	2.3 ± 0.6†	1.9 ± 0.3†
Weighted mean ± SE	0.032 ± 0.0062	0.024 ± 0.0066		
Infected (high)				
Rh 1314	0.015 (0.013–0.069)	0.014 (0.013–0.056)	1.5	1.3
Rh 1316	0.044 (0.035–0.056)	0.044 (0.037–0.053)	1.9	2.9
Rh 1292	0.058 (0.050–0.081)	0.093 (0.070–0.124)	2.0	2.5
Rh 1442	0.029 (0.026–0.050)	0.034 (0.031–0.050)	2.9	3.4
Rh 1284	0.022 (0.020–0.039)	0.026 (0.023–0.043)	2.2	2.6
Rh 1296	0.146 (0.109–0.758)	0.063 (0.047–0.085)	3.9	2.3
Rh 1348	0.093 (0.067–0.133)	0.063 (0.049–0.076)	4.3	2.5
Mean ± SE	0.058 ± 0.0177†	0.048 ± 0.0102†	2.7 ± 0.4†	2.5 ± 0.2†
Weighted mean ± SE	0.033 ± 0.0092	0.043 ± 0.0083		

*Measured by the SIV bDNA assay (P. Dailey, Chiron) and expressed as RNA copies per volume. †Significantly different from the uninfected group ($P < 0.05$) by the t-test. ‡Calculated by weighting each value by the factor $\alpha_i = (1/\sigma_i^2)/(\Sigma_i\ 1/\sigma_i^2)$, where σ_i is the bootstrap estimate of the SE (*29*). To calculate the SE of the weighted mean, we used a random-effects model to account for both the variability of the least-squares estimate measured by bootstrap and the random variability among animals.

populations turned over faster than $CD45RA^+$ subpopulations, consistent with conclusions drawn previously from results generated in mice (*17*) and humans (*18, 19*) by diverse experimental approaches. In addition, for each cell population studied, the mean values also showed that cell turnover was substantially higher in SIV-infected macaques than in normal macaques. This conclusion is again consistent with the "generalized activation" state that has been previously described, largely on the basis of surface-phenotype studies, for HIV-1 and SIV infection (*20*).

For $CD3^+$ $CD4^+$ T cells in normal monkeys, $p = 0.001$ day^{-1} is equivalent to a doubling time of ~700 days, whereas $d = 0.010$ day^{-1} is equivalent to a half life of ~70 days [see (*21*) for comparison with previous estimates for humans]; for infected monkeys with high viral load, $p = 0.031$ day^{-1} is equivalent to a doubling time of 22 days, whereas $d = 0.058$ day^{-1} is equivalent to a half-life of 12 days (*22*). When these values of p and d as well as the baseline CD4 lymphocyte counts were used to calculate the average daily turnover rates for the $CD3^+CD4^+$ population per macaque (*23*), a proliferation rate of 3.6×10^7 cells/day and a death rate of 3.6×10^8 cells/day was obtained for normal animals; corresponding proliferation and death rates in infected macaques with high viral load were 4.0×10^8 cells/day and 7.5×10^8 cells/day, respectively. If extrapolation of these results to humans is appropriate, each of these rates would be multiplied by approximately 10 to account for the size difference. The difference between the death rate and the proliferation rate equals the input of cells from the source (*11*), also known as the replacement rate. The mean daily replacement rates for $CD3^+CD4^+$ and $CD3^+CD4^-$ lymphocytes in uninfected macaques were 0.9% and 1.0%, respectively (Table 1), which are compatible with the reported T cell replacement rate in normal mice of about 1% per day (*17*). The replacement rates were approximately two- to threefold higher in SIV-infected macaques.

Thus, SIV infection was associated with a heightened lymphocyte turnover. Proliferation rates in $CD4^+$ and $CD8^+$ T lymphocytes were markedly elevated in infected macaques, although these estimates have large coefficients of variation; corresponding death rates, which have considerably smaller coefficients of variation, show in-

Table 2. Mean downslope ± SE of the exponential decay of BrdU-labeled cells (day^{-1}) in various lymphocyte subpopulations.

Labeled cells	Macaques		
	Uninfected	Infected (low)	Infected (high)
$CD3^+CD4^+$			
$CD45RA^-$	0.013 ± 0.004	0.030 ± 0.005*	0.040 ± 0.004*
$CD45RA^+$	<0.001 ± 0.005	0.011 ± 0.004*	0.014 ± 0.003*
$CD3^+CD4^-$			
$CD45RA^-$	0.020 ± 0.003	0.036 ± 0.005*	0.039 ± 0.004*
$CD45RA^+$	0.005 ± 0.002	0.013 ± 0.003*	0.020 ± 0.002*
$CD3^-CD8^+CD16^+$	0.012 ± 0.002	0.016 ± 0.003*	0.027 ± 0.005*
$CD3^-CD20^+$	0.032 ± 0.005	0.037 ± 0.004	0.056 ± 0.005*

*Significantly different from the uninfected group ($P < 0.05$).

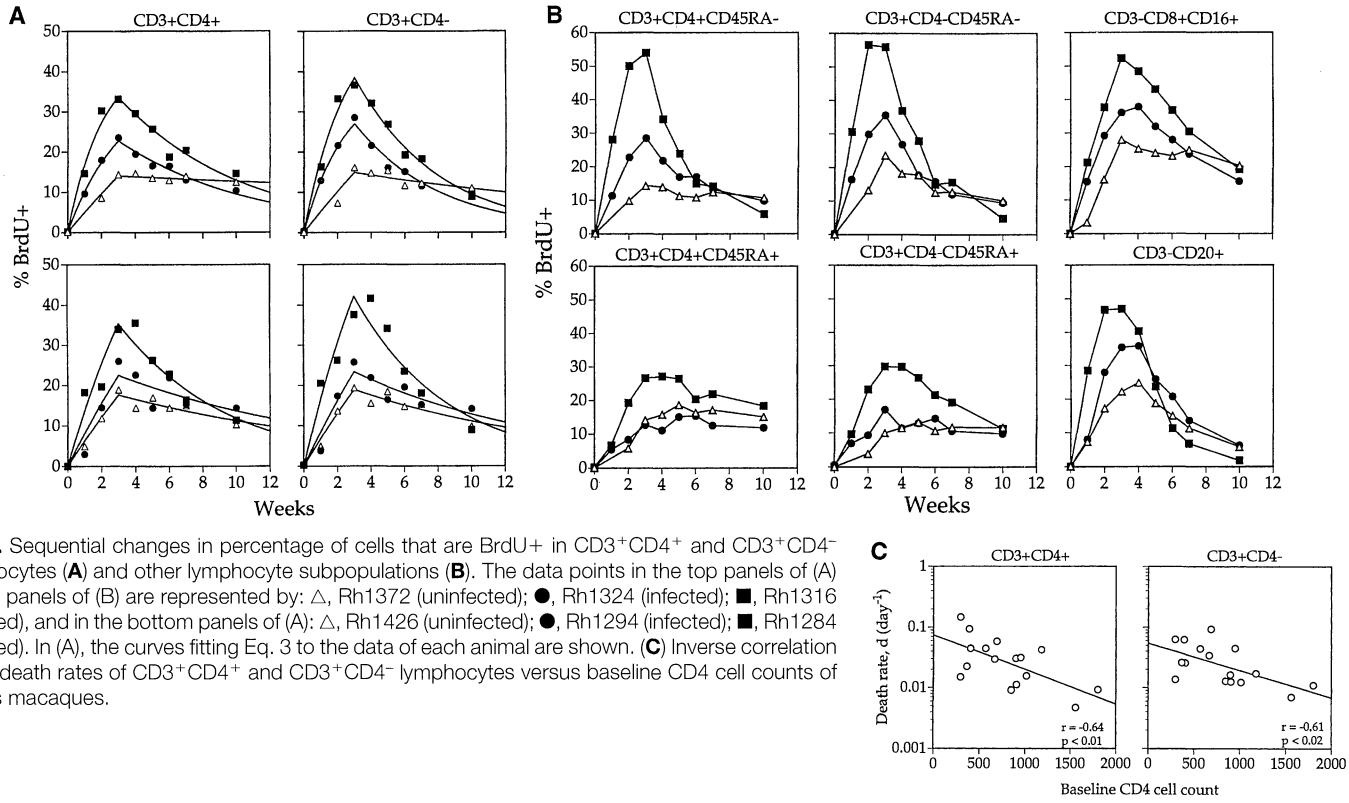

Fig. 1. Sequential changes in percentage of cells that are BrdU+ in $CD3^+CD4^+$ and $CD3^+CD4^-$ lymphocytes (**A**) and other lymphocyte subpopulations (**B**). The data points in the top panels of (A) and all panels of (B) are represented by: △, Rh1372 (uninfected); ●, Rh1324 (infected); ■, Rh1316 (infected), and in the bottom panels of (A): △, Rh1426 (uninfected); ●, Rh1294 (infected); ■, Rh1284 (infected). In (A), the curves fitting Eq. 3 to the data of each animal are shown. (**C**) Inverse correlation of the death rates of $CD3^+CD4^+$ and $CD3^+CD4^-$ lymphocytes versus baseline CD4 cell counts of rhesus macaques.

creases of 2.3- to 5.8-fold (Table 1). Furthermore, a lower baseline CD4 T cell count was correlated with a faster death rate in T lymphocytes (Fig. 1C).

That the lymphocyte turnover is increased by SIV infection is consistent with numerous observations reported in HIV-1 infection, including higher lymphocyte expression of activation markers (*20*), cell-cycling antigens (*24*), and markers of apoptosis (*25*). However, our results here directly contradict the conclusion drawn by Wolthers *et al.* (6). Given the definitive demonstration of a higher lymphocyte turnover by our study, the lack of telomere shortening in CD4 T cells found in some studies (6, *26*) could be reinterpreted to suggest a selective elimination of rapidly proliferating cells by HIV-1.

These results raise a number of questions. Is the generalized activation of T and B lymphocytes and NK cells driven by antigens produced by the persistently active infection, or, as has been described for other viral infections (*27*), is it mediated by cytokines induced by the replicating virus? Our findings here demonstrate that CD4 and CD8 lymphocytes are turning over in parallel, with similar rates. Why then is CD4 T cell depletion observed and not CD8 T cell depletion, at least not until the preterminal stage of HIV-1 infection? Is the reserve for CD8 lymphocytes actually larger? Moreover, what mechanism of cell killing could be envisioned to account for the comparable death rates of CD4 and CD8 lymphocytes in an infection caused by a virus that is only infectious and cytopathic for $CD4^+$ cells? Could the apoptosis that follows generalized activation be the principal contributor to cell killing? Finally, what makes up for the large difference between death and proliferation rates for each of the lymphocyte populations in our macaques (Table 1)? How likely is it that the thymus serves as this large source given that adult thymic capacity is generally quite low (*28*)? Could there be an extrathymic source elsewhere which could continuously supply new cells to maintain the dynamic equilibrium (*11*)? Answers to these questions could shed light not only on the pathogenesis of immunodeficiency viruses but also on normal T cell homeostasis.

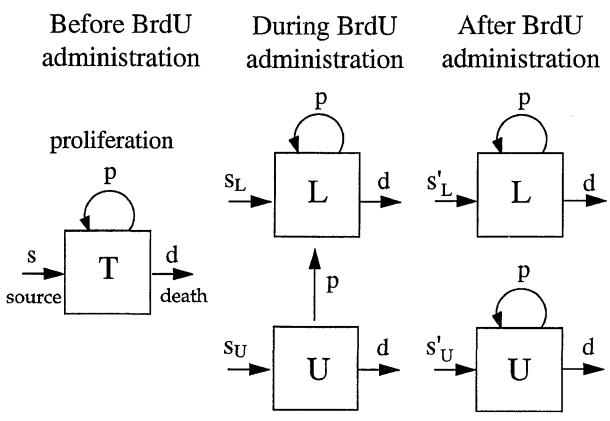

Fig. 2. Schematic representation of the mathematical model. All terms are defined in the text, except for T, the total cell population, which is at all times equal to $U + L$. The source represents input of cells from a number of possibilities (*11*).

REFERENCES AND NOTES

1. D. D. Ho *et al.*, *Nature* **373**, 123 (1995); X. Wei *et al.*, *ibid.*, p. 117.
2. M. A. Nowak *et al.*, *J. Virol.* **71**, 7518 (1997).
3. A. S. Perelson, A. U. Neumann, M. Markowitz, J. M. Leonard, D. D. Ho, *Science* **271**, 1582 (1996); A. S. Perelson *et al.*, *Nature* **387**, 188 (1997).
4. J. Sprent and D. Tough, *Nature* **375**, 194 (1995); D. E. Mosier, *ibid.*, p. 193; D. S. Dimitrov and M. A. Martin, *ibid.*, p. 194.
5. Z.-Q. Zhang *et al.*, *Proc. Natl. Acad. Sci. U.S.A.*, **95**, 1154 (1998); A. Lafeuillade *et al.*, *J. Infect. Dis.* **176**, 1378 (1997).
6. K. C. Wolthers *et al.*, *Science* **274**, 1543 (1996).
7. Surface staining of lymphocytes was performed using anti-monkey CD3-biotin (BioSource International), anti-human CD4-APC (Exalpha), anti-human CD45RA–RD-1 (Coulter), anti-human CD16-PE (Coulter), and anti-CD20 (Becton Dickinson). Anti-human CD8-APC (Caltag) was used on occasion. Additional antibodies that are normally used to characterize human lymphocyte subpopulations were

not used because of their poor reactivity with rhesus lymphocytes.
8. After surface staining, cells were treated with FACS Lysing Solution (Becton Dickinson) for 15 min at room temperature, followed by overnight fixation in 1% paraformaldehyde and 0.05% NP-40 in phosphate-buffered saline (PBS) at 4°C. Cellular DNA was then denatured with 50 Kunitz units of DNase-I (Boehringer Mannheim) for 30 min at 37°C, before staining with anti-BrdU (Becton Dickinson) in 5% fetal bovine serum and 0.5% NP-40 in PBS for 45 min. Cells were washed twice before flow cytometric analysis.
9. H. Mohri and D. D. Ho, data not shown.
10. J. Sprent and D. F. Tough, *Science* **265**, 1395 (1994); B. Rocha *et al.*, *Eur. J. Immunol.* **20**, 1697 (1990); P. Carayon and A. Bord, *J. Immunol. Methods* **147**, 225 (1992).
11. This model assumes that the average rates of cell proliferation and death are constant, as are the source rates, during labeling and delabeling. Although the source may represent cells being exported from the thymus or extrathymic tissues, which are expected to label rapidly with BrdU, it could also include a population of resting or slowly dividing T cells, which upon activation would undergo rapid clonal expansion and enter the subpopulation of cells acquiring label during the experiment. Indeed, we have developed a model based on such a mechanism, which provides the source while explaining the observed findings (S. Bonhoeffer and A. Perelson, unpublished results).
12. The assumption that labeling is 100% efficient so that the progenies of all dividing cells become labeled can be relaxed. Let ε be the fraction of unlabeled cells that fail to label on division. Eq. 1 then becomes $dU/dt = s_U + \varepsilon pU - (1 - \varepsilon)pU - dU$ and $dL/dt = s_L + 2(1 - \varepsilon)pU + pL - dL$, with solution $f_L(t) = C(1 - e^{-C2t})$, where $C = 1 - s_U/U(0)C_2$ and $C_2 = (1 - 2\varepsilon)p + d$. If $\varepsilon = 0$, then all cells label on division, and Eqs. 1a and 1b are retained.
13. After a sufficient number of cell divisions following the removal of BrdU, some cells may have so little label in them that they are not distinguishable from unlabeled cells. We ignored this possible means of loss of labeled cells, because a close examination of our BrdU-intensity data did not reveal any substantially lower values with the passage of time.
14. The constant $C = 1 - s_U/[U(0)(p + d)]$, where $U(0)$ is the number of unlabeled cells at the start of the experiment. Biologically, the way to think about C is that if there is no source of unlabeled cells during the labeling phase of the experiment, then in principle, all cells would become labeled if BrdU were administered long enough. In such a scenario, $C = 1$. If $C < 1$, it suggests that unlabeled cells are being generated, either because labeling is inefficient or because there is an unlabeled resting pool of cells that may be activated into division. During the delabeling phase, the actual solution of Eq. 2 is $f_L(t) = [f_L(T) - C_1]e^{-(d-p)(t-T)} + C_1$, where $C_1 = s'_L/[U(0)(d - p)]$. We have chosen to neglect C_1 in Eq. 3 for three reasons. First, including C_1 and then using nonlinear regression to estimate C_1, we find $C_1 = 0$ in some cases. Second, when the estimate of C_1 is not zero, we find there is no statistically significant increase in the ability of the model to fit the data. Third, at long times, $f_L(t)$ approaches C_1. However, our data suggest that at long times, especially in infected animals, the fraction of labeled cells is very small.
15. Upon activation, CD45RA$^+$ cells convert to CD45RA$^-$ cells, and reversion of CD45RA$^-$ cells to CD45RA$^+$ cells has also been shown (*10, 17*). Thus, a more complicated model is required to analyze the data. We have been unable to fit the results to the equations describing the complicated model, in part because of the introduction of several additional unknown parameters (conversion rates). However, if little conversion is assumed to occur during the course of this 10-week experiment, Eq. 3 can be used to model the CD45RA$^+$ and CD45RA$^-$ populations.
16. Data points from weeks 3 through 10 were fitted to a straight line by linear regression. If the conversions between subpopulations are small or nonexistent, then the downslope equals $(d - p)$.
17. D. F. Tough and J. Sprent, *J. Exp. Med.* **179**, 1127 (1994).
18. N.-P. Weng, B. L. Levine, C. H. June, R. J. Hodes, *Proc. Natl. Acad. Sci. U.S.A.* **92**, 11091 (1995).
19. A. R. McLean and C. A. Michie, *Ibid.*, p. 3707; C. A. Michie, A. McLean, C. Alcock, P. C. L. Beverley, *Nature* **360**, 264 (1992).
20. J. V. Giorgi and G. Janossy, *AIDS* **8** (suppl. 1), S183 (1994); H. C. Lane *et al.*, *N. Engl. J. Med.* **309**, 453 (1983).
21. McLean and Michie (*19*) estimated that in humans, $p = 0.00078$ day^{-1} in unprimed cells (CD45RA$^+$), that $p = 0.00650$ day^{-1} in primed cells (CD45RO$^+$), and that $d = 0.00014$ day^{-1}. Our estimate of p, which is for the total CD4 population, lies between their estimates for the primed and unprimed populations. However, our estimate of d is substantially larger, perhaps because of the fact that McLean and Michie analyzed cross-sectional data obtained from patients rebuilding their lymphocyte pool after radiotherapy, who may indeed have had very low T cell death rates. Our data reflect a pool of cells that acquired label during the experiment. This may be a subset of lymphocytes that turn over more rapidly than the total population.
22. Doubling time = $\ln 2/p$; half-life = $\ln 2/d$.
23. Conversion to absolute rates of CD3$^+$CD4$^+$ lymphocyte proliferation and death was based on (p or d) × (baseline CD4 cell count/μl) × (~550 ml of total blood volume) × 50. The last number adjusts for the fact that the total body lymphocyte pool is ~50 times larger than that in blood.
24. N. Sachsenberg *et al.*, in preparation; D. Tse and D. D. Ho, unpublished observation.
25. L. Meyaard *et al.*, *Science* **257**, 217 (1992); M. L. Gougeon *et al.*, *J. Immunol.* **156**, 3509 (1996).
26. L. D. Palmer *et al.*, *J. Exp. Med.* **185**, 1381 (1997).
27. D. F. Tough, P. Borrow, J. Sprent, *Science* **272**, 1947 (1996).
28. C. L. Mackall *et al.*, *N. Engl. J. Med.* **332**, 143 (1995).
29. B. Efron and R. Tibshirani, *Stat. Sci.* **1**, 54 (1986).
30. We thank P. Marx for advice, J. Mittler and C. Macken for discussions and assistance with data analysis, A. Gettie, W. Chen, J. Ko, and P. Dailey for technical help, and J. Mahoney for performing the biopsies. The experimental protocol was reviewed and approved by our institutional animal care and use committee, and humane treatment of macaques was carried out in accordance with institutional guidelines. Supported by grants from NIH (AI40387, AI41534, AI45218, AI38573, and RR06555), The Wellcome Trust, and the Irene Diamond Fund.

7 October 1997; accepted 15 January 1998